Available online at www.sciencedirect.com
ScienceDirect
Journal of Molecular Catalysis A: Chemical 284 (2008) 1–7
JOURNAL OF MOLECULAR CATALYSIS A: CHEMICAL
www.elsevier.com/locate/molcata

Catalytic hydrogenation of phenyl aldehydes using bimetallic Pt/Pd and Pt/Au nanoparticles stabilized by cubic silsesquioxanes

Xiuli Li [a], Baozong Li [a], Manhuan Cheng [a], Yukou Du [a], Xiaomei Wang [b], Ping Yang [a,*]

[a] College of Chemistry and Chemical Engineering, Suzhou 215123, Suzhou University, China
[b] College of Materials Science and Engineering, Suzhou 215123, Suzhou University, China

Received 25 August 2007; received in revised form 7 December 2007; accepted 11 December 2007
Available online 27 December 2007

Abstract

Pt/Pd and Pt/Au bimetallic nanoparticles stabilized by octa(diacetic aminophenyl)silsesquioxanes (OAAPS) were prepared and used as catalysts for hydrogenation of phenyl aldehydes to phenyl alcohols with dihydrogen under mild conditions. Transmission electron microscopy (TEM), X-ray diffraction (XRD), and UV–vis absorption spectroscopy showed that nearly monodisperse nanoparticles having average diameters of 2.6 ± 0.5 and 3.1 ± 0.7 nm for Pt/Pd and Pt/Au bimetallic nanoparticles formed. The colloidal solution of the bimetallic nanoparticles stabilized by OAAPS is stable without precipitation for 3 months at room temperature since OAAPS can offer strong bonding to the bimetallic nanoparticles through the chelating effect. Pt/Pd bimetallic nanoparticles stabilized by OAAPS showed much higher catalytic activity for the hydrogenation of phenyl aldehydes to phenyl alcohols than their monometallic counterparts. The Pd atoms in Pt/Pd nanoparticles promoted the activity of the catalytic hydrogenation mainly through geometric and electronic effects. The bimetallic nanoparticles stabilized by OAAPS can be separated from the reaction system and reused by simply adjusting the pH of the colloidal solution.

Keywords: Pt/Pd and Pt/Au bimetallic nanoparticles; Octa(diacetic aminophenyl)silsesquioxanes; Catalytic hydrogenation; Phenyl aldehydes

1. Introduction

Bimetallic nanoparticles have attracted much attention since many of them lead to interesting size-dependent optical and magnetic properties [1–3]. Bimetallic nanoparticles are particularly important in the field of catalysis because the interactions between the two components in bimetallic nanoparticles introduce a mutual influence on the neighboring atoms, which leads to unique electronic and structural properties of the nanoparticles and improves catalytic activity of monometallic nanoparticles [4–15]. However, metallic nanoparticles are unstable and have a tendency to agglomerate, thus causing the loss of their catalytic activity. In order to preserve the finely dispersed state of nanoparticles at synthetic and catalytic stages, organic polymers such as polyvinylpyrrolidinone [15,16] are usually used as stabilizers. In recent years, dendrimers have been considered as a new type of stabilizer or template for metallic nanoparticles because of their well-defined structures and chemical versatility [17–19]. Since Vögtle and co-workers reported the first synthesis of poly(propyleneimine) dendrimers in 1978 [20], many different dendrimers such as poly(amidoamine), polyaryl ether, and polyhedral oligomeric silsesquioxanes dendrimers have been successfully synthesized [21–24]. Using dendrimers as ligands, stabilizers or templates, various metallodendrimers, monometallic and bimetallic nanoparticles have been successfully synthesized. These organometallic dendrimers and dendrimer-stabilized metal nanoparticles proved to be efficient catalysts for Heck reaction, shape-selective epoxidation, alkene oxidation, Kharasch addition reaction, cyclocarbonylation, olefin hydroformation, and asymmetric and symmetric hydrogenations [24–45]. Among these dendrimers, polyhedral oligomeric silsesquioxanes have been recognized as nice stabilizers since they offer strong bonding to metal nanoparticles due to chelation. Cole-Hamilton's group reported a number of rhodium metallodendrimers based on polyhedral oligomeric silsesquioxane cores that showed unusual selectivity and the positive dendritic effect in the hydroformylation reactions [24,46–48]. We have reported preparation and

* Corresponding author. Tel.: +86 512 65880361; fax: +86 512 65880089.
E-mail address: pyang@suda.edu.cn (P. Yang).

1381-1169/$ – see front matter © 2007 Elsevier B.V. All rights reserved.
doi:10.1016/j.molcata.2007.12.023

catalysis of platinum nanoparticles stabilized by octa(diacetic aminophenyl)silsesquioxanes (OAAPS). The Pt nanoparticles stabilized by OAAPS were active and quite stable for catalytic hydrogenations [45].

In this paper, we report the preparation of bimetallic nanoparticles (Pt/Pd and Pt/Au) stabilized by OAAPS and the application of these bimetallic nanoparticles as catalysts for the hydrogenation of phenyl aldehydes to phenyl alcohols. The Pt/Pd bimetallic nanoparticles in molar ratio of two to one were highly active for phenyl aldehydes hydrogenation catalysis at ambient conditions. The high catalytic activity of Pt/Pd bimetallic nanoparticles can be attributed to a synergy between platinum and palladium of the nanoparticles.

2. Experimental

2.1. Materials

H_2PtCl_6 (A. R.), $HAuCl_4$ (A. R.), K_2PdCl_4 (A. R.), benzaldehyde (A. R.), 3-phenoxybenzaldehyde (A. R.), and organic solvents were purchased from Shanghai Chemical Reagents Company. All the chemical reagents were used without further purification. The synthesis and characterization of octa(diacetic aminophenyl)silsesquioxanes (OAAPS) were described in Ref. [45].

2.2. Preparation of monometallic and bimetallic nanoparticles stabilized by OAAPS

Monometallic nanoparticles of platinum, gold, and palladium stabilized by OAAPS were synthesized by an ethanol reduction method [49]. In this process, the alcohol acts both as solvent and reducing agent. In a typical experiment, 4×10^{-3} mmol H_2PtCl_6 and 0.133×10^{-3} mmol OAAPS were mixed with 20 mL aqueous alcohol solution ($EtOH/H_2O = 1.5$ v/v) at pH 9–10. The solution was heated to reflux for 2 h, resulting in a monometallic colloidal solution. Bimetallic nanoparticles stabilized by OAAPS were prepared by the co-reduction of H_2PtCl_6 and K_2PdCl_4 (or $HAuCl_4$) in the presence of OAAPS. A mixture of H_2PtCl_6 and K_2PdCl_4 (or $HAuCl_4$) was added to an aqueous ethanol solution of OAAPS. The molar ratio of the total metal to OAAPS was fixed to 30:1. The solution was heated to reflux under vigorous stirring. After the color of the solution changed from light orange to dark brown, the solution was cooled down to room temperature and continued to be stirred for another hour with bubbling hydrogen gas into the solution. For convenience, the samples were labeled as $Pt_{30-x}Pd_x$@OAAPS, and $Pt_{30-x}Au_x$@OAAPS, where x varies between 0 and 30.

2.3. Characterization

UV–vis absorption spectra were recorded on a TU1810 SPC spectrophotometer. X-ray diffraction (XRD) patterns were obtained with a Philips diffractometer using Ni-filtered Cu Kα radiation. Transmission electron microscopy (TEM) studies were conducted on a TECNAI-G20 electron microscope operating at an accelerating voltage of 200 kV. The samples for TEM analysis were prepared by dropping ca 3 μL of the dilute colloidal solution onto a Formvar-covered copper grid and drying in air at room temperature. X-ray photoelectron spectroscopy (XPS) experiments were carried out on a RBD upgraded PHI-5000C ESCA system (Perkin Elmer) with Mg Kα radiation ($h\nu = 1253.6$ eV). The X-ray anode was run at 250 W and the high voltage was kept at 14.0 kV with a detection angle at 54°. The pass energy was fixed at 46.95 eV. The samples for XPS analysis were prepared by dropping the bimetallic colloidal solution on Si wafers (8 mm × 8 mm), dried in vacuum and placed into a desiccator filled with hydrogen prior to the measurements. The base pressure of the analyzer chamber was about 5×10^{-8} Pa. Binding energies were calibrated by using the containment carbon (C1s = 284.6 eV).

2.4. Catalytic hydrogenation of phenyl aldehydes

Hydrogenation reactions were carried out in a 50 mL three-necked, round-bottomed Schlenk flask equipped with a hydrogen adapter, a dropping funnel, and a reflux condenser with a second adapter connected to a liquid paraffin bubbler. The system was purged with H_2 for 30 min before the reaction. Reactions were carried out by adding 2 mmol of substrate dissolved in 16 mL EtOH–H_2O solvent ($EtOH/H_2O = 1$ v/v) and 4×10^{-3} mmol of a monometallic or bimetallic colloid as the catalyst through the drop funnel under vigorous stirring conditions. Using the mixed EtOH–H_2O as a solvent for the reaction is that they are not only safe for the human health but also can maintain a homogeneous reaction mixture during the catalytic hydrogenation process. The reaction product was analyzed by GC-9800 gas chromatography equipped with an FID detector and a capillary column (Alpha-Col 30QC3/AC20). The reduction process of the substrates can also be monitored conveniently through the descending of the absorption peak centered at 306 nm. The relative error of the two methods is less than 2%. All of the hydrogenation reactions were carried out at 40 °C and atmospheric pressure.

3. Results and discussion

Fig. 1 presents the UV–vis spectra of the solution of OAAPS, the mixture of H_2PtCl_6 and OAAPS, and Pt monometallic nanoparticles stabilized by OAAPS. The aqueous ethanol solution of OAAPS demonstrates a weak absorption peak at 245 nm (Fig. 1a). The UV–vis spectrum of the solution of H_2PtCl_6 and OAAPS mixture shows a band centered at 260 nm, which can be assigned to a ligand-to-metal charge transfer (LMCT) of $PtCl_6^{2-}$ ions (Fig. 1b). After the solution was refluxed for ca 1 h, the color of the solution changed from light orange to dark brown. The UV–vis spectrum of the solution revealed that the band at 260 nm disappeared, indicating that the $PtCl_6^{2-}$ ions were completely reduced to the zero valence metal. The solution of Pt nanoparticles stabilized by OAAPS is characterized by a monotonically increasing absorbance at decreasing wavelengths (Fig. 1c).

The UV–vis spectrum of Pd nanoparticles stabilized by OAAPS (Fig. 2a) has features that are similar to the physical mixture of Pt and Pd nanoparticles (Fig. 2c). The absorbance

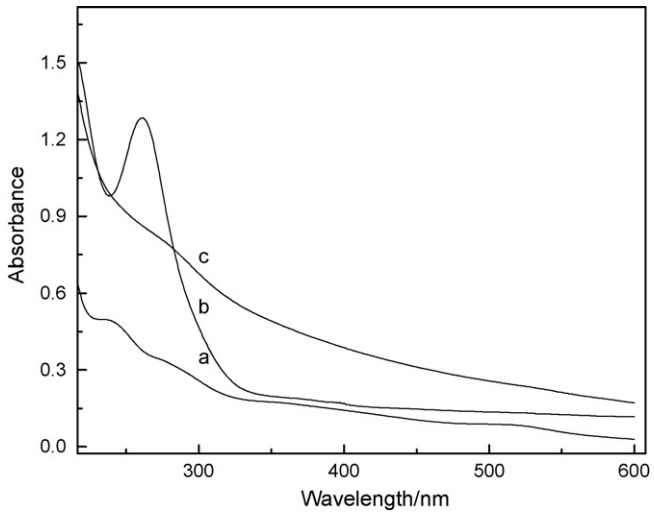

Fig. 1. UV–vis spectra of OAAPS dissolved in aqueous ethanol solution (a), the mixture of OAAPS and H_2PtCl_6 (b), and Pt nanoparticles stabilized by OAAPS (c).

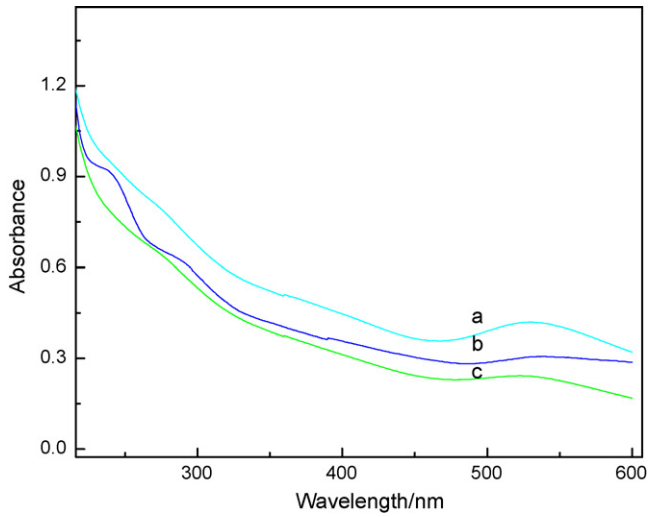

Fig. 3. UV–vis spectra of Au nanoparticles stabilized by OAAPS (a), Pt/Au bimetallic nanoparticles (b), and the physical mixture of Pt and Au monometallic nanoparticles (c). $n_{Pt}/n_{Au} = 1$; $n_{Pt+Au} = 30$.

of bimetallic Pt/Pd nanoparticles (Fig. 2b) is between Pd and the mixture of Pt and Pd nanoparticles with a monotonically increasing absorbance toward higher energies.

The brown-reddish Au colloidal solution exhibited a characteristic absorption band centered at near 520 nm (Fig. 3a), which was consistent with the surface plasmon resonance (SPR) arising from Au nanoparticles larger than 2 nm [19]. The absorption spectrum of the physical mixture of Au and Pt nanoparticles (Fig. 3c) has similar features as that of the Au colloidal solution with relative low absorbance in the measured wavelength range. The UV–vis spectrum of Pt/Au bimetallic nanoparticles (Fig. 3b) is different from that of the physical mixture of Pt and Au with a relatively high absorbance toward lower energies, which can be attributed to the dielectric function change caused by two different metal atoms mixing [50].

The XRD patterns of Pt and Pd monometallic nanoparticles (Fig. 4a and b) revealed that both of them essentially were in the face-centered cubic (fcc) structure ($2\theta = 39.7°$, 46.2° for Pt and $2\theta = 40.9°$, 46.7° for Pd). For the physical mixture of Pt and Pd nanoparticles (the molar ratio is one), the two characteristic peaks of Pt ($2\theta = 39.7°$) and Pd ($2\theta = 40.9°$) were clearly discernible (Fig. 4c). However, the two peaks merged into a broad one for the Pt/Pd (1/1) bimetallic nanoparticles (Fig. 4d). Gold monometallic nanoparticles exhibited characteristic diffraction peaks at 38.1°, 44.3°, and 64.5° corresponding to (1 1 1), (2 0 0), and (2 2 0) surfaces diffractions of the nanocrystallite (Fig. 5a). The characteristic peaks of Pt and Au can also be observed from the diffraction pattern of the physical mixture of Pt and Au monometallic nanoparticles (Fig. 5b). The observed reflections of Pt/Au bimetallic nanoparticles are clearly different from

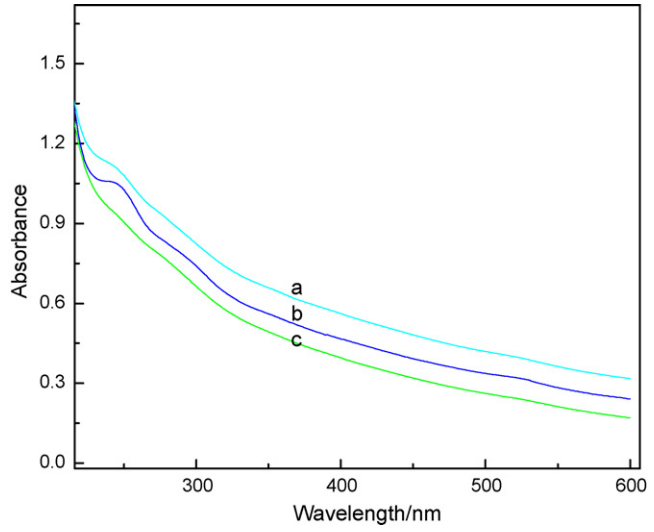

Fig. 2. UV–vis spectra of Pd nanoparticles stabilized by OAAPS (a), Pt/Pd bimetallic nanoparticles stabilized by OAAPS (b), and the physical mixture of Pt and Pd monometallic nanoparticles (c). $n_{Pt}/n_{Pd} = 1$; $n_{Pt+Pd} = 30$.

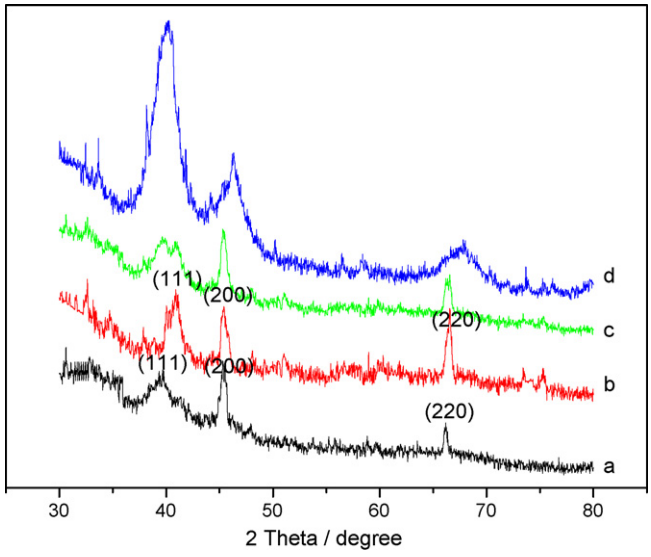

Fig. 4. XRD patterns of Pt nanoparticles (a), Pd nanoparticles (b), the physical mixture of Pt and Pd nanoparticles (c), and Pt/Pd bimetallic nanoparticles stabilized by OAAPS (d).

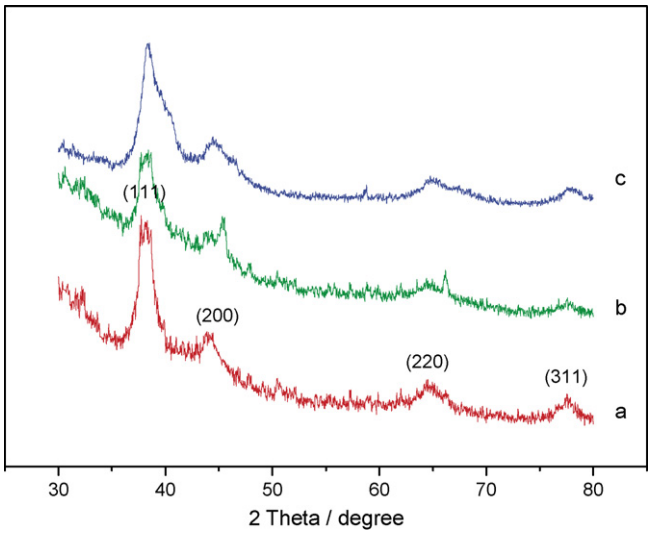

Fig. 5. XRD patterns of Au nanoparticles (a), the physical mixture of Pt and Au nanoparticles (b), and Pt/Au bimetallic nanoparticles stabilized by OAAPS (c).

those of the physical mixture of the Pt and Au monometallic nanoparticles. The XRD pattern of Pt/Au bimetallic nanoparticles (Fig. 5c) revealed that the very close two peaks existing in the pattern of the mixture of the Pt and Au monometallic nanoparticles were replaced by a broad peak. The fact that the XRD patterns of bimetallic combinations show broad bands while their monometallic counterparts exhibit fairly sharp peaks provides nice evidence of the formation of bimetallic nanoparticles [51].

Transmission electron microscopy (TEM) images of the bimetallic nanoparticles stabilized by OAAPS and the corresponding size histograms are presented in Fig. 6. As shown by the TEM micrographs, the shape of these bimetallic nanoparticles is basically spherical. The Pt/Pd bimetallic nanoparticles display near-monodisperse and the average diameter of the nanoparticles is 2.6 ± 0.5 nm (Fig. 6a). The Pt/Au bimetallic nanoparticles exhibit a relatively wide-size distribution (1.5–4.5 nm); the average diameter and dispersivity obtained from the histogram plot are 3.1 ± 0.7 nm (Fig. 6b). The colloidal solution of the bimetallic nanoparticles stabilized by OAAPS is stable without precipitation for at least 3 months at room temperature since OAAPS can offer strong bonding to

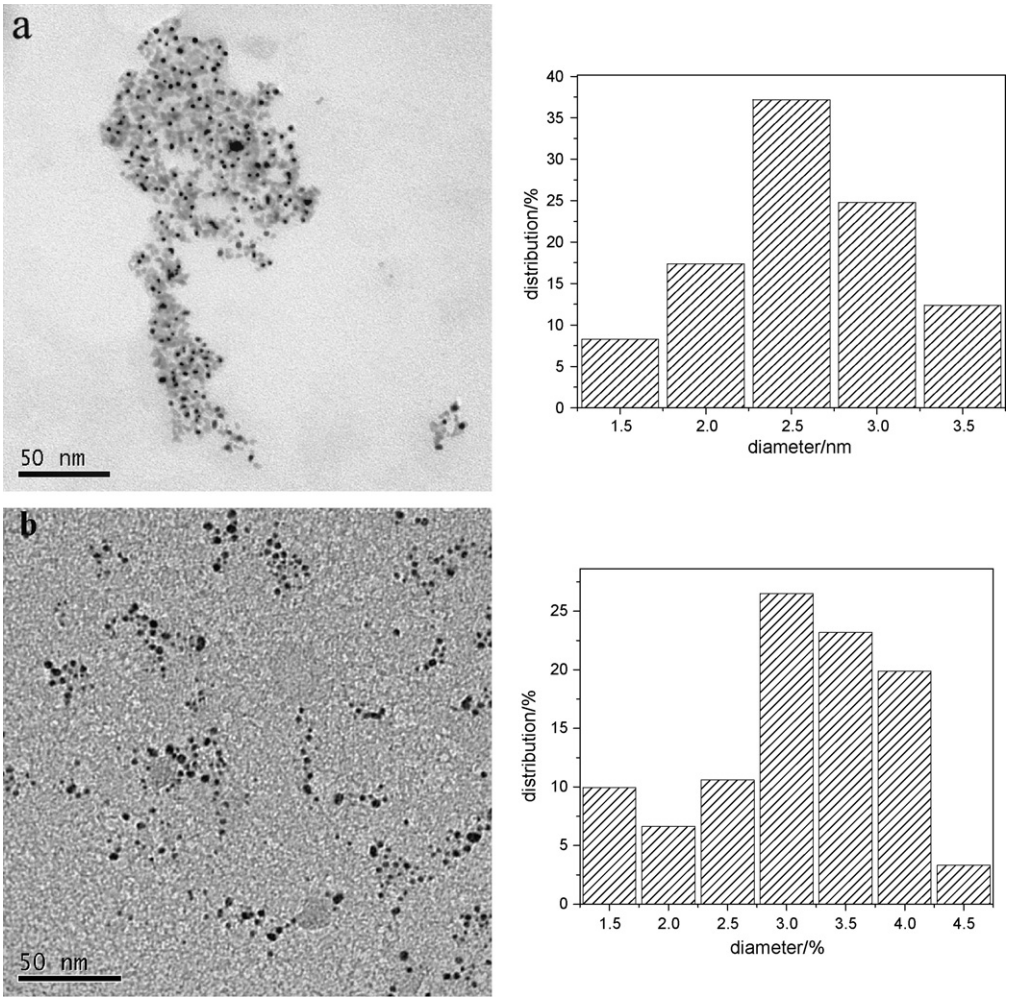

Fig. 6. Transmission electron micrographs of bimetallic nanoparticles. The average size and standard deviation of the particles are 2.6 ± 0.5, and 3.1 ± 0.7 nm for Pt/Pd@OAAPS (a), Pt/Au@OAAPS (b) nanoparticles. The samples were prepared in the conditions: $n_{Pt}/n_{M2} = 1{:}1$, $n_{metal}/n_{OAAPS} = 30$.

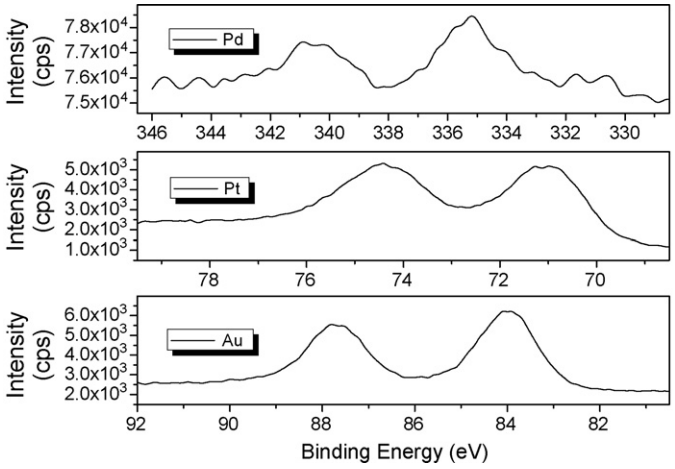

Fig. 7. XP spectra of bimetallic nanoparticles.

the metal nanoparticles through the chelating effect. The formation of these relative monodisperse bimetallic nanoparticles demonstrates the effectiveness of OAAPS as a stabilizer for the preparation of bimetallic nanoparticles.

The results of XP spectra of the bimetallic nanoparticles are shown in Fig. 7. The peaks corresponding to metallic palladium $3d_{5/2}$ and $3d_{3/2}$ levels are observed at 335.3 and 340.6 eV binding energies, respectively. Similarly, platinum $4f_{7/2}$ and $4f_{5/2}$ peaks appear at 71.1 and 74.4 eV, while gold $4f_{7/2}$ and $4f_{5/2}$ peaks are observed at 84.0 and 87.7 eV, respectively. The results of XPS investigations indicate the formation of zero valent bimetallic nanoparticles [52].

The hydrogenation of 3-phenoxy-benzaldehyde (POBAD) was chosen to be the model reactions to investigate the catalytic activities of as-prepared bimetallic nanoparticles since the hydrogenation product 3-phenoxy-benzalcohol of POBAD is an important material for medicine and pesticide. The catalytic hydrogenation activities of benzaldehyde catalyzed by the nanoparticles were also investigated for comparison. The selectivities of phenyl alcohols at the end of hydrogenation were higher than 99%. Results about the catalytic hydrogenation of benzaldehyde and 3-phenoxy-benzaldehyde are summarized in Table 1.

As shown in Table 1, using Pt monometallic nanoparticles as the hydrogenation catalyst, the conversations of benzaldehyde and 3-phenoxy-benzaldehyde are 45.9% and 29.5% in 2 h reaction, respectively. Pd monometallic nanoparticles show relatively high catalytic hydrogenation activity to benzaldehyde (70.2% in 2 h) and relatively low activity to 3-phenoxy-benzaldehyde (17.9% in 2 h). Pt/Pd bimetallic nanoparticles show higher catalytic activity than their monometallic counterparts. Using Pt_{20}/Pd_{10} nanoparticles as the hydrogenation catalyst, the conversions of benzaldehyde and 3-phenoxy-benzaldehyde in 2 h reach 99.4% and 92.6%, respectively. The Pt/Pd ratio of bimetallic nanoparticles influences the catalytic activity but is dependent on the substrates. As the Pt/Pd molar ratio of Pt/Pd bimetallic nanoparticles varied from 2 to 0.5, the conversion of 3-phenoxy-benzaldehyde in two hours' reaction decreased from 92.6% to 77.7%; while for benzaldehyde hydrogenation the catalytic activity only decreased slightly. The different catalytic activities of the nanoparticles to the substrates may be attributed to the different molecular structures of the substrates. Benzaldehyde is the simplest aromatic aldehyde that can penetrate the stabilizer shell of the nanoparticles easily to the catalytic moiety; while the access of 3-phenoxy-benzaldehyde to the catalytic sites of the nanoparticles is relatively difficult, since 3-phenoxy-benzaldehyde has a relatively large molecular size. In addition, the electronic effect of the phenoxy group at *meta*-position of the substrate may also reduce its hydrogenation activity. The enhanced catalytic activity of the bimetallic nanoparticles may be explained as an ensemble effect of platinum and palladium. However, which one of the two metals acted as a main active phase in the bimetallic catalyst still needs investigation.

The influences of the reaction temperature and molar ratio of substrate to catalyst on the catalytic activity are shown in Fig. 8. The substrate conversion decreases with the increase of the molar ratio of POBAD to catalyst (Fig. 8a). The catalytic activity of the bimetallic nanoparticles increases as the reaction temperature increases from 25 °C to 40 °C, then decreases as the temperature is beyond 40 °C (Fig. 8b). The fact that the catalytic activity decreases at higher reaction temperature maybe attributed to the partial pressure of dihydrogen decreases as the pressure of the

Table 1
Catalytic activity of monometallic and bimetallic nanoparticles for hydrogenation of phenyl aldehydes to phenyl alcohols

Catalyst	Conversion of BAD in 2 h (%)	Conversion of POBAD in 2 h (%)
Pt_{30}@OAAPS	45.9	29.5
Pt_{20}/Pd_{10}@OAAPS	99.4	92.6
Pt_{15}/Pd_{15}@ OAAPS	98.8	83.0
Pt_{10}/Pd_{20}@OAAPS	98.7	77.7
Pd_{30}@OAAPS	70.2	17.9
Pt_{20}/Au_{10}@OAAPS	–	22.8

Reaction conditions: solvent:ethanol/water = 1 (v/v); $n_{substrate}/n_{catalyst} = 500$; reaction temperature: 40 °C.

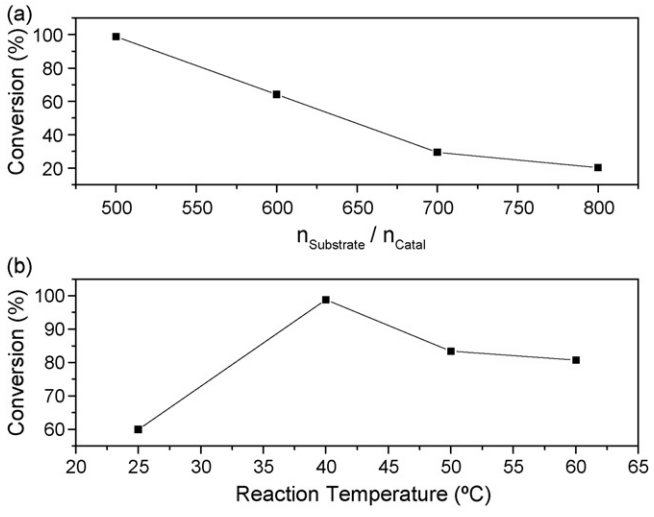

Fig. 8. Influences of reaction temperature and molar ratio of substrate to catalyst on the catalytic activity.

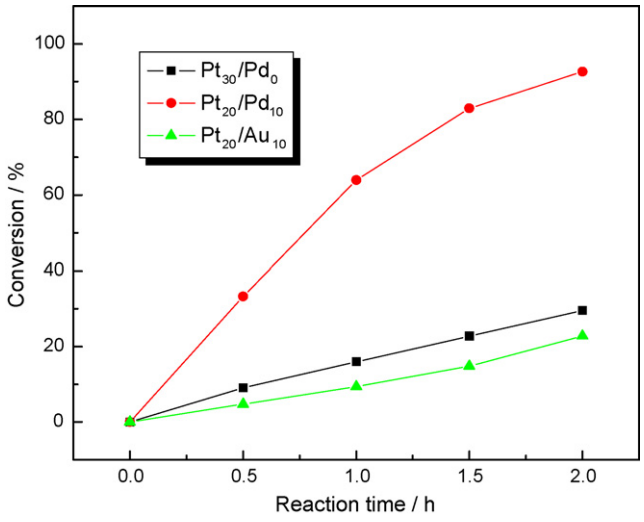

Fig. 9. Catalytic hydrogenation of 3-phenoxy-benzaldehyde by different catalysts. *Reaction conditions*: $n_{metal}/n_{OAAPS} = 30$; solvent:ethanol/water = 1 (v/v); $n_{substrate}/n_{catalyst} = 500$; reaction temperature: 40 °C.

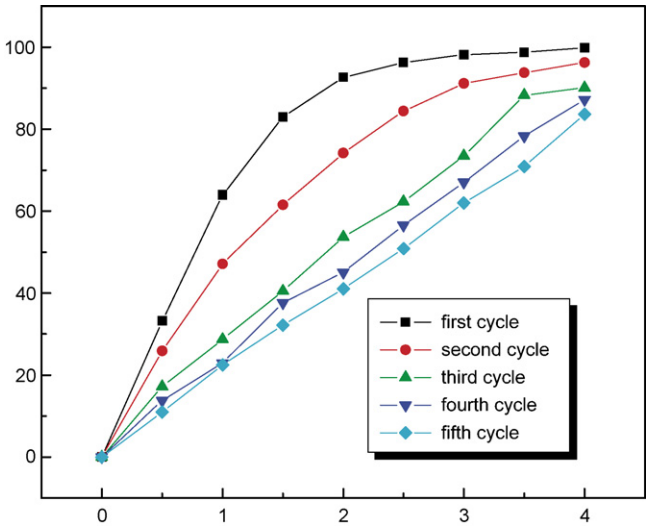

Fig. 10. Pt_{20}/Pd_{10}@OAAPS catalyst recycling for hydrogenation of 3-phenoxy-benzaldehyde. *Reaction conditions*: $n_{metal}/n_{OAAPS} = 30$; solvent:ethanol/water = 1 (v/v); $n_{substrate}/n_{catalyst} = 500$; reaction temperature: 40 °C.

mixed solvent increases with raising the reaction temperature since the system is maintained at atmospheric pressure.

The conversions of 3-phenoxy-benzaldehyde catalyzed by Pt monometallic nanoparticles, Pt_{20}/Pd_{10}, and Pt_{20}/Au_{10} bimetallic nanoparticles versus reaction time are shown in Fig. 9. The results demonstrate that the activity of Pt_{20}/Au_{10} nanoparticles is relatively lower than that of Pt monometallic nanoparticles, but much lower than that of Pt_{20}/Pd_{10} bimetallic nanoparticles. In general, it is believed that the introduction of the second metallic element varies the configuration and the electronic structure of the nanoparticles that consequently lead to different catalytic behaviors [53].

The catalytic activity of bimetallic nanoparticles is also influenced by the molar ratio of the total metal to the stabilizer in nanoparticles. Generally, the catalytic activity of bimetallic nanoparticles increases with the increasing ratio of the total metal to OAAPS, since there will be more surface of the bimetallic nanoparticles unpassivated for catalysis at a larger ratio of the metal to the stabilizer. In our experiments, the bimetallic nanoparticles were stable for the catalytic hydrogenation when the molar ratio of the total metal to OAAPS is 30. Beyond the value, the agglomeration of the bimetallic nanoparticles is obvious.

Like their monometallic counterparts, bimetallic nanoparticles stabilized by OAAPS can also be precipitated by adjusting the solution to acidic [45]. The precipitated bimetallic nanoparticles can be redissolved in a slightly basic aqueous ethanol solvent by ultrasonic treatment. This provides a convenient method of recycling the catalyst. The catalytic activity of Pt_{20}/Pd_{10}@OAAPS bimetallic nanoparticles decreased obviously in the second and the third cycle, while in the following cycles the catalytic activity dropped slightly (Fig. 10). The phenomenon may be explained that some vertex or edge atoms of the nanoparticles, which may compose catalytic sites, might move to the more stable surface during the reaction and recycling process and the migration might level off after these cycles. However, Pt/Pd bimetallic nanoparticles still exhibited nice activity for 3-phenoxy-benzaldehyde catalytic hydrogenation, even when recycled five times.

4. Conclusions

Pt/Pd and Pt/Au bimetallic nanoparticles were successfully prepared using octa(diacetic aminophenyl)silsesquioxanes as the stabilizer. The Pt/Pd bimetallic nanoparticles show an excellent catalytic activity for the hydrogenation of phenyl aldehydes to phenyl alcohols compared to the monometallic platinum or palladium nanoparticles. Meanwhile the unprotected Pt/Pd bimetallic suspension for the catalytic hydrogenation only shows low catalytic activity under the same reaction conditions since the agglomeration of particles takes place. Pd in Pt/Pd bimetallic nanoparticles stabilized by OAAPS promoted catalytic activity through an ensemble effect. The bimetallic nanoparticles catalysts stabilized by OAAPS can be recycled by simply adjusting the pH of the solution.

Acknowledgement

The authors gratefully acknowledge the financial support of the National Natural Science Foundation of China (20673075 and 50673070).

References

[1] H. Zhang, D.E. Zelmon, L.G. Deng, H.K. Liu, B.K. Teo, J. Am. Chem. Soc. 123 (2001) 11300.
[2] Ch.J. O'Connor, J.A. Sims, A. Kumbhar, V.L. Kolesnichenko, W.L. Zhou, J.A. Wiemann, J. Magn. Magn. Mater. 226–230 (2001) 1915.
[3] J. Dai, Y. Du, F. Wang, P. Yang, Physica E 39 (2007) 271.
[4] J. Sinfelt, Acc. Chem. Res. 20 (1987) 134.
[5] O.S. Alexeev, B.C. Gates, Ind. Eng. Chem. Res. 42 (2003) 1571.
[6] R. Raja, J.M. Thomas, J. Mol. Catal. A: Chem. 181 (2002) 3.

[7] B.F.G. Johnson, S.A. Raynor, D.B. Brown, D.S. Shephard, T. Mashmeyer, J.M. Thomas, S. Hermans, R. Raja, G. Sankar, J. Mol. Catal. A: Chem. 182/183 (2002) 89.
[8] B. Veisz, L. Tóth, D. Teschner, Z. Paál, N. Győrffy, U. Wild, R. Schlögl, J. Mol. Catal. A: Chem. 238 (2005) 56.
[9] L. Guczi, A. Beck, A. Horváth, Zs. Koppány, G. Stefler, K. Frey, I. Sajó, O. Geszti, D. Bazin, J. Lynch, J. Mol. Catal. A: Chem. 204/205 (2003) 545.
[10] S.N. Pronkin, P.A. Simonov, V.I. Zaikovskii, E.R. Savinova, J. Mol. Catal. A: Chem. 265 (2007) 141.
[11] Y.M. Chung, H.K. Rhee, J. Mol. Catal. A: Chem. 206 (2003) 291.
[12] A. Villa, C. Campione, L. Prati, Catal. Lett. 115 (2007) 133.
[13] M.O. Nutt, K.N. Heck, P. Alvarez, M.S. Wong, Appl. Catal. B Environ. 69 (2006) 115.
[14] R. Scott, A. Datye, R. Crooks, J. Am. Chem. Soc. 125 (2003) 1757.
[15] P. Lu, T. Teranishi, K. Asakura, M. Miyake, N. Toshima, J. Phys. Chem. B 103 (1999) 9673.
[16] R. Narayanan, M.A. El-Sayed, J. Am. Chem. Soc. 125 (2003) 8340.
[17] D. Astruc, F. Chardac, Chem. Rev. 101 (2001) 2991.
[18] G. Newkome, E. He, C. Moorefield, Chem. Rev. 99 (1999) 1689.
[19] R. Scott, O. Wilson, R. Crooks, J. Phys. Chem. B 109 (2005) 692.
[20] E. Buhleier, W. Wehner, F. Vögtle, Synthesis (1978) 155.
[21] D.A. Tomalia, A.M. Naylor, W.A. Goddard III, Angew. Chem., Int. Ed. Engl. 29 (1990) 138.
[22] G. Newkome, Z. Yao, G.R. Baker, V.K. Gupta, J. Org. Chem. 50 (1985) 2003.
[23] C.J. Hawker, J.M.J. Fréchet, J. Am. Chem. Soc. 112 (1990) 7638.
[24] L. Ropartz, R.E. Morris, D.F. Foster, D.J. Cole-Hamilton, Chem. Commun. (2001) 361.
[25] Y. Niu, L. Yeung, R. Crooks, J. Am. Chem. Soc. 123 (2001) 6840.
[26] K. Esumi, R. Isono, T. Yoshimura, Langmuir 20 (2004) 237.
[27] E. Rahim, F. Kamounah, J. Frederiksen, J. Christensen, Nano Lett. 1 (2001) 499.
[28] K. Gopidas, J. Whitesell, M. Fox, Nano Lett. 3 (2003) 1757.
[29] R. Scott, A. Datye, R. Crooks, J. Am. Chem. Soc. 125 (2003) 3708.
[30] F. Gröhn, B.J. Bauer, Y.A. Akpalu, C.L. Jackson, E.J. Amis, Macromolecules 33 (2000) 6042.
[31] M. Zhao, R. Crooks, Angew. Chem., Int. Ed. 38 (1999) 364.
[32] M. Ooe, M. Murata, T. Mizugaki, K. Ebitani, K. Kaneda, Nano Lett. 2 (2002) 999.
[33] M. Zhao, R. Crooks, J. Am. Chem. Soc. 120 (1998) 4877.
[34] P. Bhyrappa, J. Young, J. Moore, K. Suslick, J. Mol. Catal. A: Chem. 113 (1996) 109.
[35] Z. Yang, Q. Kang, H. Ma, C. Li, Z. Lei, J. Mol. Catal. A: Chem. 213 (2004) 169.
[36] G. Koten, J. Jastrzebski, J. Mol. Catal. A: Chem. 146 (1999) 317.
[37] R. Touzani, H. Alper, J. Mol. Catal. A: Chem. 227 (2005) 197.
[38] Y. Huang, H. Zhang, G. Deng, W. Tang, X. Wang, Y. He, Q. Fan, J. Mol. Catal. A: Chem. 227 (2005) 91.
[39] T. Mizugaki, M. Ooe, K. Ebitani, K. Kaneda, J. Mol. Catal. A: Chem. 145 (1999) 329.
[40] G. Smith, S. Mapolie, J. Mol. Catal. A: Chem. 213 (2004) 187.
[41] B. Yi, Q. Fan, G. Deng, Y. Li, L. Qiu, A. Chan, Org. Lett. 6 (2004) 1361.
[42] Y. Du, W. Zhang, X. Wang, P. Yang, Catal. Lett. 107 (2006) 177.
[43] P. Yang, W. Zhang, Y. Du, X. Wang, J. Mol. Catal. A: Chem. 260 (2006) 4.
[44] W. Zhang, Y. Du, N. Hua, X. Wang, P. Yang, Chin. J. Inorg. Chem. 22 (2006) 263.
[45] X. Li, Y. Du, J. Tao, X. Wang, P. Yang, Catal. Lett. 118 (2007) 151.
[46] L. Ropartz, D.F. Foster, R.E. Morris, A.M.Z. Slawin, D.J. Cole-Hamilton, J. Chem. Soc., Dalton Trans. (2002) 1997.
[47] L. Ropartz, R.E. Morris, D.F. Foster, D.J. Cole-Hamilton, J. Mol. Catal. A: Chem. 182/183 (2002) 99.
[48] L. Ropartz, K.J. Haxton, D.F. Foster, R.E. Morris, A.M.Z. Slawin, D.J. Cole-Hamilton, J. Chem. Soc., Dalton Trans. (2002) 4323.
[49] N. Toshima, M. Kuriyama, Y. Yamada, H. Hirai, Chem. Lett. (1981) 793.
[50] K. Torigoe, Y. Nakajima, K. Esumi, J. Phys. Chem. 97 (1993) 8304.
[51] S. Devarajan, P. Bera, S. Sampatha, J. Colloid Interface Sci. 290 (2005) 117.
[52] C. Wagner, W. Riggs, L. Davis, J. Moulder, Handbook of X-ray Photoelectron Spectroscopy, Perk-Elmer Co., Minnesota, 1979.
[53] W. Tian, M. Ge, F. Gu, T. Yamada, Y. Aoki, J. Phys. Chem. A 110 (2006) 6285.